Monatshefte für Chemie 136, 1071–1085 (2005)
DOI 10.1007/s00706-005-0286-y

Monatshefte für Chemie
Chemical Monthly
Printed in Austria

New Keys for Old Keywords. Case Studies within the Updated Paradigms of the Hybridization and Aromaticity

Fanica Cimpoesu[1,*], **Kimihiko Hirao**[2], **Marilena Ferbinteanu**[3], **Yutaka Fukuda**[4], and **Wolfgang Linert**[5]

[1] Institute of Physical Chemistry, Bucharest 77208, Romania
[2] University of Tokyo, Department of Applied Chemistry, School of Engineering, Tokyo 113-8656, Japan
[3] University of Bucharest, Faculty of Chemistry, Inorganic Chemistry Department, Bucharest 70254, Romania
[4] Ochanomizu University, Faculty of Science, Department of Chemistry, Tokyo 112-8610, Japan
[5] University of Technology, Institute of Applied Synthetic Chemistry, A-1060 Vienna, Austria

Received September 29, 2004; accepted October 12, 2004
Published online April 25, 2005

Summary. The recovery of the basic qualitative concepts of the chemical language into the quantum treatment is a rather challenging problem because the desirable simplicity is easily lost in the black box of technical mechanisms of computation, *e.g.* among the ingredients of post-orbital methods of correlation effects. We present here several clues for bringing the hybridization and aromaticity concepts in a nontrivial and non-redundant conjunction with both quantum chemical quantities and the chemists' tools of intuition. A rather inedited structural correlation that works as an experimental proof of the hybridization is discussed. The main idea is to exploit the intermediate symmetries, where the hybridization is no longer tautological because of the symmetry. For instance in a MA_2B_2 tetrahedron, if the hybridization not existed as real engine of the stereochemistry, the AMA and BMB angles should be arbitrarily independent. In turn, if the hybridization acts, there is a certain trigonometric relationship between the two angles. The existence of this correlation is noticed and discussed in prototypic series. A new understanding and analysis of strain in cycles and clusters (with particular emphasis on organometallic structures) is constructed as continuation of discussed models. The problem of aromaticity in chelates, rings and clusters is approached by means of specific models. The careful attention devoted to the structural details rewards the theory with an extended understanding of various bonding regimes and at the same time enriches the experimentalists' perspectives beyond the geometric description and taxonomic systematization of X-ray molecular structure and crystal packing data.

* Corresponding author. E-mail: cfanica@yahoo.com

Keywords. Hybridization; Aromaticity; *Ab Initio*; Curved Bond; Coordination Compounds; Clusters.

Introduction

In the early ages of theoretical chemistry, *R. S. Mulliken* noticed the ongoing tendency that "*the more accurate the calculations become, the more the concepts tend to vanish into thin air*" [1]. Indeed, with the advent of modern methods, algorithms, computer software, and hardware helping the theory of bonding, the thesaurus of qualitative ideas like hybridization, hypervalence, electronegativity, aromaticity, *etc.*, became of rather secondary use for the theoretical chemistry itself. Such concepts changed their status from the initial *a priori* explanatory virtues, expressing the active causal agents, to the rather passive role as subject of the eventual *a posteriori* recovery from the bare output of the electronic structure methods. Since the first principles are now perceived as incorporated in the *ab initio* methods themselves, most often the qualitative lexicon appeared superfluous with respect of the ways and tasks of computational chemistry. Also it is definitely not easy to extract from routine outputs the information directly matching the major keywords. However, the terms of the above invoked paradigms still form the basis in which the chemists from the experimental branches of synthetic chemistry and physicochemical measurements can understand and handle the basic theoretical information, for the sake of routine explanation or partial prediction. Therefore, revisiting the basic keys for unlocking the technically inherent language gate between pure computational chemistry and the pure experimental one, serves to the very practical purposes of interlocking unitary frames, contributing to a renewed *Organon* for the whole chemistry.

There are several modern tools affording valuable translation of the wavefunction information into chemically meaningful language. Without attempting an exhaustive list of theories or procedures with such virtues, we will briefly outline here the Natural Bond Orbital (NBO) method [2] due to *Weinhold et al.*, the Atoms in Molecules (AIM) [3], *Bader*'s theory, and the Charge Density Analysis (CDA) [4] of Frenking. Alternate access to heuristic interpretation is gained by nonstandard handling of the *ab initio* data, *e.g.* arranging them in the terms of *Heisenberg-Dirac van Vleck Hamiltonian*, as is the *Malrieu*'s approach to the polyenes [5] and bond-alternation distortions [6]. We will do in the following a selective walk among concepts and procedures outlining the link between the calculation data [7] and the chemical concepts.

Results and Discussion

The Hybridization

The hybridization is one of the simplest ideas of the bonding. This simplicity may keep away the theoretical attention, but given its large popularity among chemists is easy to advocate reasons for a deeper insight. In fact, the hybridization is one way to account for the so-called local character of the correlation effects [8]. Especially in systems with firm chemical bonds, the major part of correlation

energy can be efficiently treated in terms of localized orbitals, to which the hybrids are good choices. There is a number of work devoted to the hybridization as semiempirical tool [9], or to its relevance in localization problems [10] as well as to the idea that, due to correlation reasons, the hybridization really works as an engine conferring supplementary stabilization to the atoms in the bond [11]. The most complete quantum approach to the hybridization is given by means of Natural Hybrid Orbitals (NHOs) in the Natural Bond Orbital (NBO) theory [2].

We will add here a new perspective to the question, outlining the non-trivial correlation that can be established between details of molecular geometry and the electronic structure in the key of quantitative approach of hybridization. The main idea is to exploit the intermediate symmetries, where the hybridization is no longer tautological because of symmetry (*e.g.* as in the pure T_d point group, where the sp^3 composition necessarily results from $a + t_2$ representation of the tetrahedron vertices). In fact, at high symmetries we do not know how much the hybridization acts as a physical force or whether it is just formal. In turn, the lower symmetries of a coordination polyhedron are revealing this measure.

Illuminating illustration is found for the case of MA_2B_2 systems with C_{2v} symmetry from tetrahedral parentage. In this case, the sp^3 status should be regarded in the sense of average, expressing the necessity of forming four σ bonds with the formal contribution of the whole valence shell. Otherwise, due to chemical non-equivalence, the M–A *vs.* M–B bonds are subjected to a differential hybridization. Namely, the proportion of *s*:*p* dedicated to a given bond may vary from the standard 1:3 of sp^3, while the average on all the σ bonds retrieves the 1:3 ratio. The hybrids obey orthonormalization relationships, and due to this conjuncture, the differential hybridization in MA_2B_2 depends only on a single mixing parameter, denoted *r* (Eq. (1)) where, $h_{a\pm} \equiv s^{2r^2}p^{4-2r^2}$ and $h_{b\pm} \equiv s^{2-r^2}p^{2+r^2}$ are the hybrids devoted to the A and B ligands, respectively. The formulas of the angles are as follows by Eq. (2).

$$|h_{a\pm}\rangle = \frac{1}{\sqrt{2}}\left(r|s\rangle + \sqrt{1-r^2}|p_z\rangle\right) \pm \frac{1}{\sqrt{2}}p_x$$
$$|h_{b\pm}\rangle = \frac{1}{\sqrt{2}}\left(\sqrt{1-r^2}|s\rangle - r|p_z\rangle\right) \pm \frac{1}{\sqrt{2}}p_y \qquad (1)$$

$$\mathrm{AMA} = \arccos\left(-\frac{r^2}{2-r^2}\right) \qquad \mathrm{BMB} = \arccos\left(-\frac{1-r^2}{1+r^2}\right). \qquad (2)$$

Since both angles are related with a single parameter, *r*, the AMA and BMB values are mutually dependent (see the curve in Fig. 1). If the hybridization does not exist as real effect, then the AMA and BMB would vary arbitrarily. In this clue we present a rather inedited structural correlation that works as an experimental proof of tetrahedral sp^3-type hybridization, at intermediate symmetries. Namely, plotting the theoretical correlation of AMA *vs.* BMB angles we found in the series $[MF_2(CH_3)_2]^-$ (M = Al, Ga, In) an almost perfect placement of experimental bond angles on the theoretical curve [12]. This series can be taken as prototype for the hybridization at the intermediate C_{2v} symmetry.

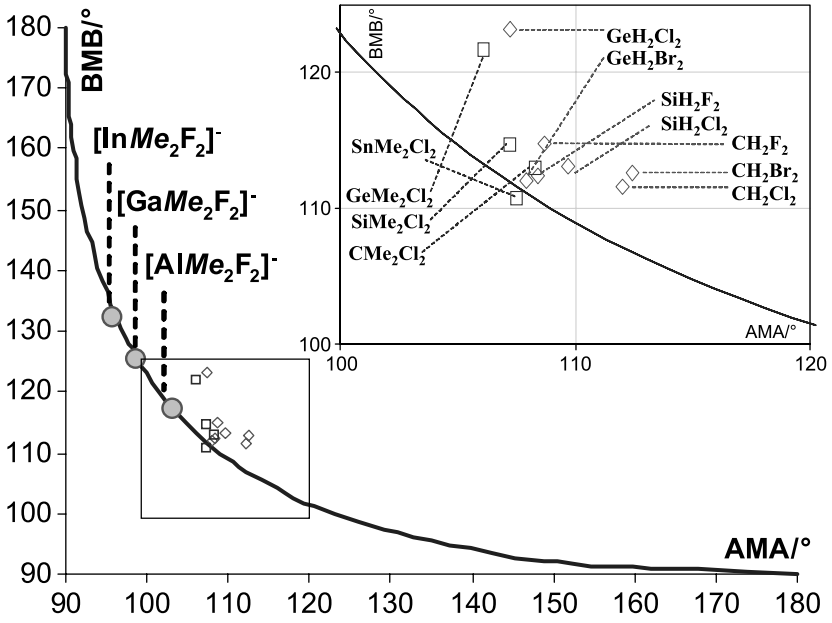

Fig. 1. The mutual correlation of AMA and BMB angles in the MA_2B_2 tetrahedra; the theoretical correlation due to differential hybridization relationships is shown as continuous line; the inset shows a magnified area including several neutral molecules with group IV central atom

We emphasize again that the correlation is not trivial and that the hybrization ideas are even more relevant at low symmetries. In this way, the hybridization can be used in a quantitative sense, stepping beyond the usual qualitative views of poor information content, in which all the tetrahedrally substituted atoms are simply sp^3 and no more.

Rather strikingly, the correlation of angles in C_{2v} molecules with carbon atoms, shown in the inset of Fig. 1, is less perfect than those of ionic metal-complexes from the main figure. The reason is that in the ionic systems, the total energy can be regarded with a good approximation as sum of atomic body energies (plus their electrostatic interaction) and then hybridization, as engine of stabilizing the central ion, determines directly the molecular shape. In covalent systems, the individual stabilization of central atom plays a smaller role, as compared to the covalence itself, making the relationship more complex.

We confined here only on C_{2v} systems. Similar constructions can be done for other symmetries. For instance, going to C_s, in a $MAA'B_2$ system, the hybrids of A and A′ differentiated ligands can be obtained by a rotation with a new parameter, t (Eq. (3)), within the $h_{a\pm}$ set from Eq. (1), while the $h_{b\pm}$ hybrids of the $\{MB_2\}$ moiety are the same as in Eq. (1).

$$|h_a\rangle = t\left(r|s\rangle + \sqrt{1-r^2}|p_z\rangle\right) + \sqrt{1-t^2}|p_x\rangle$$
$$|h_{a'}\rangle = \sqrt{1-t^2}\left(r|s\rangle + \sqrt{1-r^2}|p_z\rangle\right) - t|p_x\rangle \qquad (3)$$

A general procedure, for a system with C_1 symmetry can be designed as follows. First produce a set on normalized, non-orthogonal functions (Eq. (4)) as

function of *Cartesian* positions of the *N* ligands, and then submit the $|\tilde{h}_i\rangle$ set to the orthogonalization, to obtain the conventional $|h_i\rangle$ hybrid set. The procedure is general also for differential hybridizations from sp^2 or *sp* parentage.

$$|\tilde{h}_i\rangle = \left(\sqrt{1 - \frac{x_i^2}{\sum_{k=1}^{N} x_k^2} - \frac{y_i^2}{\sum_{k=1}^{N} y_k^2} - \frac{z_i^2}{\sum_{k=1}^{N} z_k^2}}\right)|s\rangle + \frac{x_i}{\sqrt{\sum_{k=1}^{N} x_k^2}}|p_x\rangle + \frac{y_i}{\sqrt{\sum_{k=1}^{N} y_k^2}}|p_y\rangle + \frac{z_i}{\sqrt{\sum_{k=1}^{N} z_k^2}}|p_z\rangle \quad (4)$$

In spite of its simplicity, the above model offers electronic structure information without performing a calculation, just exploiting the angular parameters, from the experimental structure. For the elements of main group it is indisputable that the *s* and *p* shells are the major content of Natural Hybrid Orbitals (NHOs from NBO procedures). The content in *d* orbitals is small, about 1–2%, negligible as factor determining the hybrid directionality, eventhough polarization functions have their precise role in improving the computed energy data, bond lengths, or other quantities. Then the *p* composition determines the lobe orientation, irrespective of their radial functions, or those of *s* type. The multiple split of the basis sets does not alter the fact that effective hybrid-like functions can be constructed and that their angular part can be anticipated from geometrical reasons. The orthonormality relationships help in the definition of hybrids as combination of effective *s* and *p* sets. The fact that we may predict the NHOs in advance of a calculation (*e.g.* within a basis of Natural Atomic Orbitals specific to a given atomic basis) can be developed into technically useful implications, for starting guess in regular computations, or in alternate techniques like the direct solving of the density matrix without diagonalization.

Particular Bonding Conditions. The Strain in the Cycles

The strained cycles, *i.e.* the rings where the geometry or symmetry imposes bond angles smaller than those allowed by regular hybridization ideas, are regarded as rather particular cases of bonding (curved bond path [13]). Choosing cycles with members of MA_2B_2 (C_{2v}) nature one may call the above hybridization formulas to measure the hybrid deviations with respect of edges. The clue is to consider that, if the A fragments belong to cycle, then for the outer M–B bonds the hybrids are free to follow the $\beta = \text{BMB}$ bond angle. With Eq. (2) we retrieve the hybridization parameter $r = \sqrt{(1 + \cos(\beta))/(1 - \cos(\beta))}$, knowing then with the help of Eq. (1) the AMA hybrid bond angle. The departure from the geometrical AMA gives the strain in the cycle, measured as the deviation: $\tau = (\text{AMA}_{\text{hybrid}}(r) - \text{AMA}_{\text{geometric}})/2$.

Considering the cyclopropane [14], as prototype of extreme strain, taking the $\beta = \text{HCH} \sim 114.5^\circ$, the corresponding $r = 0.625$ shows that the hybrids toward the cycle must have 105.12°, with a deviation $\tau = 22.56^\circ$ from the geometrical $\text{CCC} = 60^\circ$ angle.

We will not discuss here the energy implications of the strain, continuing with the analysis of angular cycle strain in rather subtle situations of inorganic rings,

where the simple intuition is helpless. Then, the quantitative view of hybridization enables a preliminary analysis. Let us take the computed $\{Me_2AlF\}_2$ molecule (by B3LYP/6-311G*) with the optimized angles FAlF = 78.95° and CAlC = 127.85.

The computed geometry of the model molecules is quite close to those of an experimental case, namely $\{Me(C_6H_2Me_3)F\}_2$ with FAlF = 77.66°, which is however slightly distorted from C_{2v} symmetry. For sake of idealization we will consider then the computed model case. The fit to CAlC angle gives $r = 0.489$, corresponding to the 97.82° angle toward the cycle, with $\tau = 9.43°$ deviation. The six-membered cycles are usually thought as not affected by strain. Proceeding as previously, for the $(Me_2AlF)_3$, the computed geometry is FAlF = 88.82°; CAlC = 117.65°. With $\tau = 6.8°$, one may see that a certain strain appears in these cycles also.

An example of hybrid deviation in clusters is offered by the hexagonal prismatic skeleton of the $(HAl)_6(NCH_3)_6$ model with D_{3h} symmetry. The experimental molecules [15] with this pattern do not obey the perfect symmetry, due to slight alteration by crystal packing. This skeleton is interesting for the fact that the NAlN angle in one hexagon is close to 120°, whereas the Al–N bond linking the two $\{Al_3N_3\}$ cycles is ∼90° to their planes. Thus the $\{AlN_3\}$ moiety would impose a sp^2 hybridization, which however does not fit the fact that the outer Al–C bond is not oriented in the corresponding plane. The system shows a case of bond directionalities that cannot be solved with aligned hybrids. In fact, the situation is of a strained sp^3 hybridization, as reveals the NBO analysis for the optimized structure, based on B3LYP/6-311G* computation. Thus, the hybrids in the hexagon are $s(24.50\%)p(74.32\%)d(1.18\%)$ whereas the one devoted to the third Al–N bond is $s(22.08\%)p(76.52\%)d(1.40\%)$. This composition is acquired on the expense of hybrid deviation, as illustrated in Fig. 2, aside to the schemes of previous examples.

Curved Coordination Bond and Misdirected Lone Pairs

The coordination analogue of curved bond is the so-called misdirected lone pair problem. Qualitative and semiempirical views offer a good documentation of the problem with respect to experimental evidences [16]. Here, we present an *ab initio* based analysis (B3LYP/6-311G*), with the help of the *Laplacian* of the electron density [3] and NBO methods. The molecular prototype, Ti(η^2-triazole)$_4$, is chosen to represent a class of systems with presumable large lone pair deviation, due to the η^2 coordinating azolato-type ligands [17]. The map of *Laplacian* in the coordina-

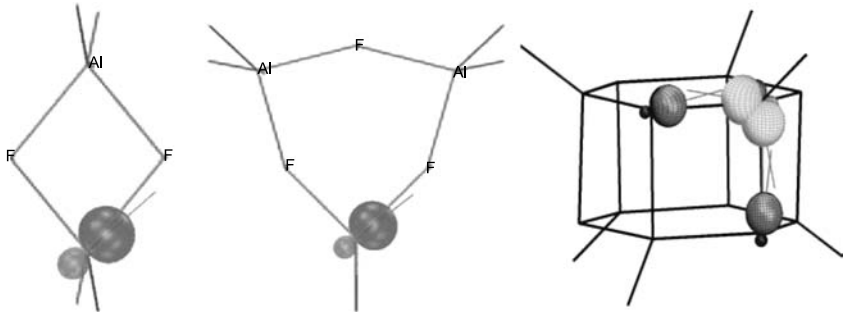

Fig. 2. Selected inorganic cycles and cluster with bond *vs*. hybrid orientation deviation

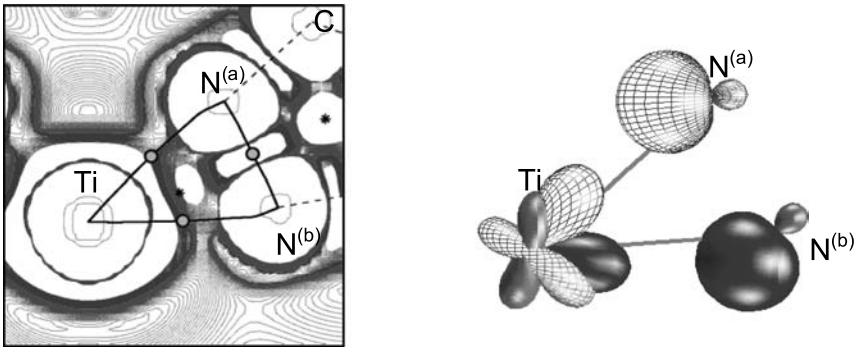

Fig. 3. *Laplacian* of electron density with bond paths (left side) and Natural Hybrid Orbitals (NHOs) for the TiNN strained chelate in the $\{TiN_8\}$ chromophore of a Ti(η^2-triazole)$_4$ complex, as illustrative case of curved coordination bond and misdirected lone pair

tion plane of one ligand proves the existence of misdirected lone pairs. As shown in Fig. 3, the lone pairs are oriented outside cycle and deformed toward the metal center. The trajectories corresponding to the so-called bond paths are showing the curved bond character of the Ti–N connections. The angle between the central atom and the (3, −1) critical points of the Ti–N bonds is definitely larger (46.39°) than the geometrical N–Ti–N angle of the optimized structure (38.73°).

Another direct image of the misdirected lone pair is obtained by NBO. As is seen in Fig. 3, both metal and ligand natural hybrid orbitals are deviated from the Ti–N axis. The opening between the maximal lobes of the metal hybrids is ∼84° whereas the geometrical N–Ti–N angle is much more acute (∼39°). The NBO analysis also reveals the ionic nature of the compound with the Ti–N bonds having 93–97% ligand character, whereas the antibonding combinations consist preponderantly of metal orbitals. Therefore, the bonding scheme follows a ligand field regime. The hybrid orbitals h_a (along upper Ti–N$^{(a)}$) and h_b (lower Ti–N$^{(b)}$) can be presented with the following formulas (Eq. (5)) where $\sigma_1 = \text{sign}(z)$ and $\sigma_2 = \text{sign}(y)$.

$$h_a = \frac{1}{2}\Big[a\cdot|s\rangle + \sqrt{1-a^2}\cdot|z^2\rangle + \sigma_1 b\cdot|z\rangle + \sigma_1\sqrt{1-b^2}\cdot|xy\rangle + \sigma_1 c\cdot(|x\rangle + \sigma_2|y\rangle) + \sigma_1\sqrt{1-c^2}\cdot(|xz\rangle + \sigma_2|yz\rangle)\Big]$$

$$h_b = \frac{1}{2}\Big[-\sqrt{1-a^2}\cdot|s\rangle + a\cdot|z^2\rangle - \sigma_1\sqrt{1-b^2}\cdot|z\rangle + \sigma_1 b\cdot|xy\rangle + \sigma_1\sqrt{1-c^2}\cdot(|x\rangle + \sigma_2|y\rangle) - \sigma_1 c\cdot(|xz\rangle + \sigma_2|yz\rangle)\Big] \quad (5)$$

Adapting the values from NBO analysis the following mixing coefficients can be presented: $a = -0.7174$, $b = 0.9756$, and $c = 0.3896$. This corresponds to the following composition of the hybrids, h_a: $s^{0.515}p^{1.26}d^{2.230}$ and h_b: $s^{0.485}p^{1.74}d^{1.770}$. The total hybridization is sp^3d^4, corresponding to the reducible representation of the Ti–N bonds in the D_{2d} reference geometry, $2a_1(s,\ d_{z^2}) + 2b_2(p_z,\ d_{xy}) + 2e([p_x, p_y],[d_{yz}, d_{xz}])$. This hybridization scheme has the same orbital and symmetry

composition as the known case of the bisdisphenoid (D_{2d} dodecahedron). However, our case represents a new pattern of the coordination number eight, not discussed before [18].

The Normal Coordination Regime. Where are the Coordinating Lone Pairs?

In the above section, the *Laplacian* analysis helped to detect the lone pairs, in accordance with the current claims of the theory of electron density descriptors [3]. We will amend here the statement, noting that in certain respects the *Laplacian* location of the lone pairs is not so visible. We considered a mixed ligand complex [19] with representative ligands, *cis*-[Co(*acac*)$_2$(*dmpz*)$_2$] (where *acac* = acetylacetonate, *dmpz* = dimethylpyrazole). The Figs. 4a and b of the ligands in the molecule show, rather surprisingly, that the lone pairs are not very prominent. The density accumulation contours assignable to the lone pairs are quite close to the nuclei, representing therefore the roots of the lone pair in the atomic cores rather than the lone pair itself.

To retrieve a better image of the coordinating lone pairs in the valence shell, further treatments must be performed. A successful one is the difference between the electron density of the ligand in complex and in the free ligand (taken in the same location and with the same geometry). In these representations the lone pair-like profiles are detected as density depression areas (dashed, light colored contours). The observation in this paragraph introduces a technical amendment to the accurate representation of lone pair ideas in coordination chemistry.

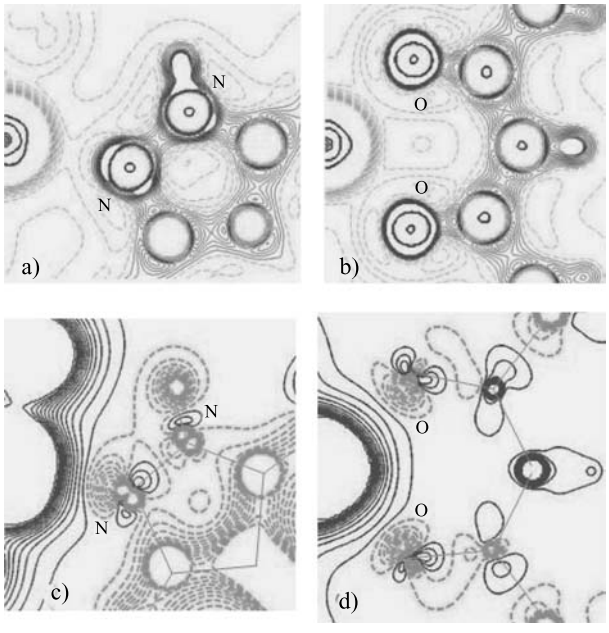

Fig. 4. The electron density descriptors applied to ligands in the complex *cis*-[Co(*acac*)$_2$(*dmpz*)$_2$]; a) and b) the *Laplacian* density maps in the coordination planes of pyrazole and acac ligands; in c) and d) the electron density difference taken as complex minus the free ligand; in all the figures the dark, continuous lines correspond to density accumulation tendency and dashed ones to depletion areas

Further surprises are revealed in the NBO frame. For acetylacetonate, the coordinating lone pairs have a content of about $s(10\%)p(90\%)$ much deviated from the $s(33\%)p(67\%)$ composition of the intuitively expected sp^2 hybrids. Besides, the coordinating hybrids are not perfectly aligned along to the Co–O axis, having a deviation of about 10° inward of the chelatic ring. An interesting situation occurs in the pyrazole ligand. Here N–Co and N–H bonds at the two nitrogen atoms provoke a rather diffuse electron density distribution along the N–N bond. This is accounted by enhancing the p content of the hybrids devoted to the N–N bond (with $p \sim 70$–80%). This occurs on the expense of other hybrids around, including the lone pair, that has available a slightly lower p content than the regular sp^2, namely $s(40\%)p(60\%)$.

Valence Bond, Spin Hamiltonian, Aromaticity and again Cycle Strain

The aromaticity is another dear keyword of the chemical language. As the collection of recent reviews in the topic shows [20], a rather large consensus appears in the computation or experimental tests for checking the presence of aromaticity (bond lengths, energy of formation, NMR shifts, and NICS indices), whereas the mechanisms themselves still remain open to the debate. The qualitative image calls the idea of resonance and technically speaking this belongs to the Valence Bond (VB) theory [21]. The VB was, on the time line, the first quantum explanation of the chemical bond. In spite of the venerable age, the VB is still theoretically actual, but moved in a back echelon due to impetus and availability of molecular orbital theories. There are modern forms of VB, *e.g.* several versions of the so-called CASVB [22, 23] combining Complete Active Space and Valence Bond techniques. However, the driving of a proper VB calculation still requires certain skills and even art of interpretation. This is because the methods of CASVB generation are even more sensitive than the CASSCF to the choice of active spaces and henceforth to the emerging physical meaning.

A phenomenological model that practically originates from the VB, the *Heisenberg-Dirac-van Vleck* (*HDVV*) [24] spin *Hamiltonian*, becomes rather popular with the wave of interest for molecular magnetism. The frequent routine use of *HDVV* to fit the magnetic susceptibility faded a bit the nature and virtues of the theory as way to interpret the chemical bond itself. Remarkable applications in the use of *HDVV* in prototypical structure and bonding problems are due to *Malrieu* [5]. Following such a conceptual line, we briefly present here a new analysis of the aromaticity, done with the help of specific developments in the *HDVV Hamiltonian*.

Without entering details, that are too technical here, being presented elsewhere [25], the short story is that, if we want accurate fit of several states, then we may need more parameters than the regular Js for each bond. The gain of more parameters by stating J values between non-neighbor, non-bonded, atoms seems a nonphysical alternative. To avoid this, but acknowledging the possibility of complex long range effects, we conceived a term that can be interpreted as the interaction between geminal bonds. As spin *Hamiltonian*, we represented such effects by intercentric spin quadratic terms. These can be regarded as a generalization of the already known one-center biquadratic ingredients, used to amend spin states

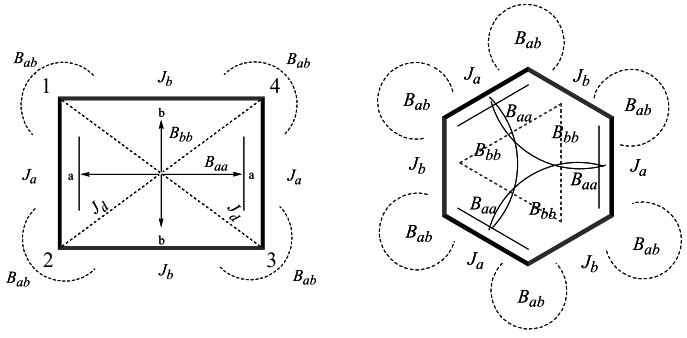

Scheme 1

spacing in certain dimers and trimers. The effective *Hamiltonian* is (Eq. (6)) were the negative *J*s give the coupling strengths of the spins into the bonds and newly introduced *B* parameters correspond to the mutual influence of the bonds. The parameters are figured in Scheme 1.

$$\hat{H} = -2\sum_{j<i}(J_{ij} + 1/2)\hat{S}_i \cdot \hat{S}_j + 8\sum_{j<i}\sum_{l<k} B_{ij,kl}(\hat{S}_i \cdot \hat{S}_j)(\hat{S}_k \cdot \hat{S}_l), \qquad (6)$$

The resonance ideas are sometime puzzling the chemists with the question of physical non-reality of separate resonance structures. In fact the resonance structures are not so ghostly. These are building blocks of the groundstate and also for one or several excited states. Formally, a proper combination of ground and excited states may define a single resonance form. In this sense of potential realization, the resonances should be regarded as fact, not fiction. Besides, in terms of π subsystem, the interactions mixing the states lead to an energy gain by the enhanced amount of configuration interaction after the symmetry lowering. In other terms, this is a case of pseudo *Jahn-Teller* effect. However the σ skeleton opposes to this distortion tendency. Considering the π system only, even the benzene would have the tendency to distort. However, its skeleton is resistant against bond alternating distortion because of good σ bonds established with the sp^2 in-plane hybrids, matching perfectly the hexagon bond angles. By contrary, the antiaromatic cyclobutadiene is frustrated in the matter of hybrid alignment along the square skeleton. The 90° bond angle can be obtained only with pure *p* orbitals. However, in this case the bond is weaker, loosing the binding effects brought by *s–p* mixing. On the other hand, the *s–p* mixing drives the hybrids non-aligned. Then, rather surprisingly, a key role in the aromaticity is played by the σ subsystem.

The fit of *HDVV* states to CASSCF(n,n/6-31G) calculations[a] ($n = 4$ for C_4H_4 and $n = 6$ for C_6H_6) afforded the *J* and *B* parameters, as function of bond alternating distortion coordinates. A term K_0 generically includes the interplay of the σ skeleton. The fitted parameters allowed the estimation of resonance energy, sub-

[a] The limitation to 6-31G basis set was done to avoid the collection of π virtual orbitals from unphysical high energy, as happens if larger *Pople* basis sets are employed, keeping then the numerical experiment closer to the pictures of intuition, with π MOs as essentially of frontier type

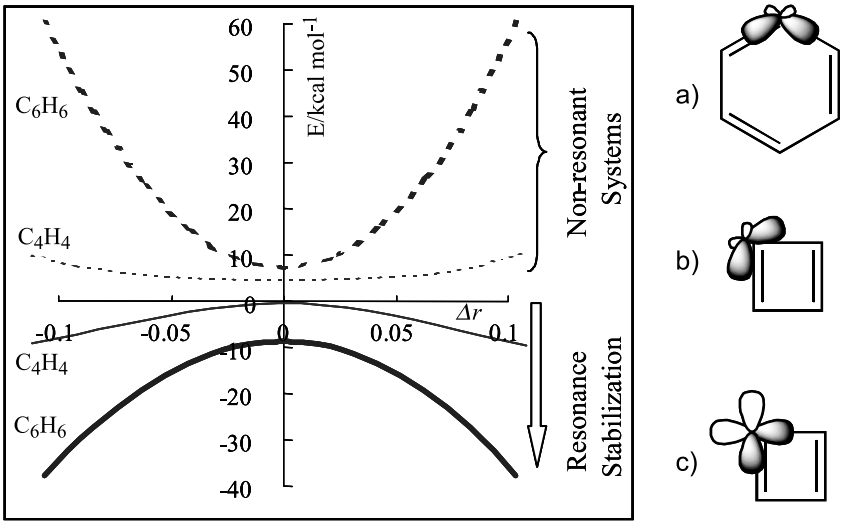

Fig. 5. The hypothetical non-resonant energy in cyclobutadiene and benzene and the corresponding resonance stabilization (in kcal/mol) obtained with the help of fitted spin *Hamiltonian* parameters (as function of bond alternating distortion)

stracting from groundstate the non-resonant energy, which is $K_0 - J_a - J_b$ for C_4H_4 and $K_0 - 3J_a/2 - 3J_b/2$ for C_6H_6. In this way we estimate for benzene a resonance stabilization of $-8.56\,\text{kcal/mol}$, comparable with the CASVB calculation [26] giving $-7.4\,\text{kcal/mol}$. Here we should note that with respect of the adopted definition and the method of estimation, the resonance energy is disputed in a very large interval (-5 to $-95\,\text{kcal/mol}$) [27].

The representation in Fig. 5 shows that the defined nonresonant superposition of states increases in energy with distortion, with a higher slope and curvature for benzene. The absolute value of resonance energy increases also with the bond-alternation distortion. This clearly emphasizes an aspect which otherwise can be confusedly understood from the usual textbook views of the problem. Namely, the resonance stabilization, as configuration interaction effect, is not a phenomenon pertaining to the symmetric structures only. It persists and even enhances with the distortion.

The Aromaticity of Coordination Chelates

The diketonates are prototypical chelating ligands. Their symmetrical geometry implies the formulation of resonance structures and therefore the presumable problem of afferent aromaticity. To address the resonance problem we will adopt here an alternative tool offered by the NBO package, the so-called Natural Resonance Theory (NRT) [28]. This method determines weights for the resonance structures, *a posteriori* to any quantum calculation (*e.g.* DFT). Note that the NRT procedure is not exactly the same thing as the resonance idea from the VB frame. However, NRT is interesting as alternative theory and besides as user friendly tool. The NRT regards the resonance as a state ensemble superposition. Then, the NRT structures are not a matter of configuration interaction, but pieces to fit the total density.

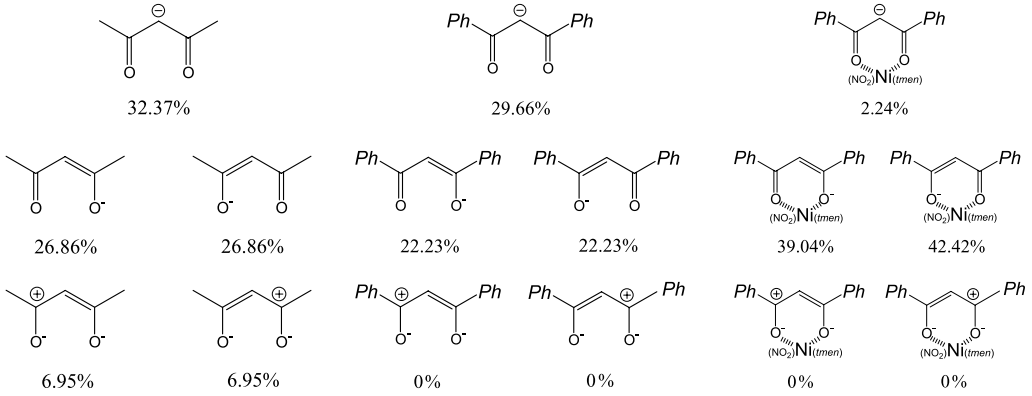

Fig. 6. The NRT resonance structure weights for free and coordinated diketonato ligands

Let us examine the NRT results for selected diketonato systems. Thus, for free acetylacetonate, the most important weights are found for keto-enolate, carbanionic, and di-enolate resonances. There are many other advanced ionic resonances (hyperconjugation-like), but with small fractions (<1%). Going to dibenzoylmethanate (*dbm*), the weights for the first three resonances are slightly lowered and the last ones completely vanished on the expense of further resonances implying conjugation with the phenyl groups. The coordinated *dbm* ligand was considered in a [Ni(*tmen*)(NO_2)(*dbm*)] mixed ligand complex [29].

The fact that the ratio of the two keto-enolate structures in the complex is raised toward the limit 50%–50% is an inedited proof of the aromaticity in these chelates. In complex, the carbanion structure is dropped to 2%, comparing with the 30% of the free anion.

The Surface Aromaticity in Clusters. A Carbalane Case Study

The idea of surface aromaticity was advanced in case of boranes and carboranes, as a structural solution accounting for electron deficiency and multicenter bonds [30]. The here discussed system is a carbalane cluster with $\{Al_8C_6\}$ cubo-octahedral pattern [31]. It showed chemical properties looking as the generalization of the aromatic ones, namely the stability of the core against the several kinds of substitutions performed to the peripheral ligands (*i.e.* a cluster behaving analogously to the benzenoid cores). In terms of electron structure, here the aromaticity can be simply explained as matter of resonance and delocalization on each Al_4C face. The delocalization of electron density enables a number of bonds which is larger than those of available lone pairs. Each Al_4C pyramidalized face contains four Al–C bonds, certified as (3, −1) critical points, while only three electron pairs are available (see Fig. 7a). Then a resonance as schematized in Fig. 7c occurs on each face.

We note that the Al_4C entities [32] are known from gas phase experiments and were also discussed in the perspective of aromaticity, on the basis of distinguished stability and orbital reasons. However, due to different electron count in the orbital scheme, the electronic structure of the neutral or ionic Al_4C species is different from that of the Al_4C fragment in the actual molecule.

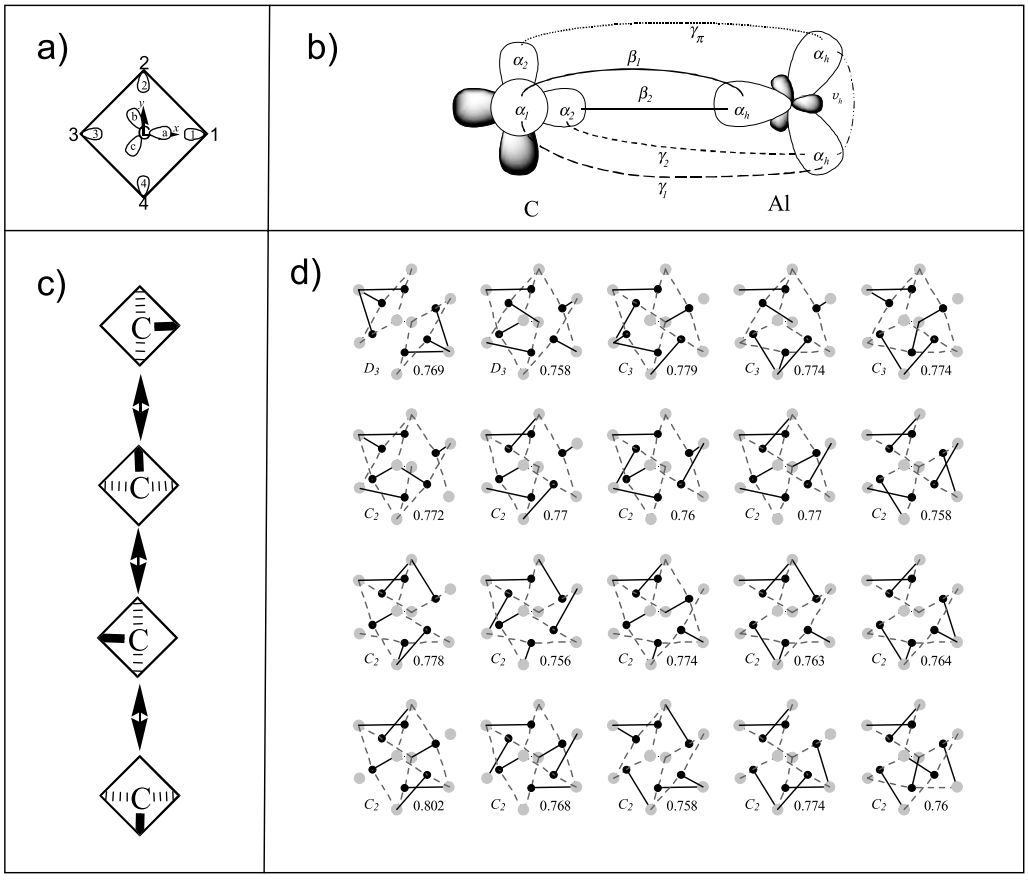

Fig. 7. a) and b) the bonding scheme for the Al_4C faces of the $\{Al_8C_6\}$ cluster; c) resonance structures at one pyramidal Al_4C face; d) selected resonances of the whole cluster

At the scale of the cluster, there are $4^6 = 4096$ resonance structures which resulted running the mentioned four possibilities on each of the six Al_4C pyramidalized faces. Several selected resonances (topologically spanning D_3, C_3, or C_2 symmetries) are presented in Fig. 7d together with the so-called TREPE index (Topological Resonance Energy Per Electron) [33].

The TREPE indices were obtained with the help of model sketching a simplified MO scheme (with 42 levels resulting from 3 AOs per atom), in terms of AOs and parameters represented in Fig. 7b. The model is of a three-dimensional *Hückel* [34] facture (not to be confused with Extended-*Hückel*). The parameters (similar to the well known α and β ones from traditional *Hückel* theory) were adjusted to reproduce the corresponding energies resulting from the B3LYP/6-311G* calculations. The obtained values are, in eV: ${\alpha_s}^M = 1.4607$, ${\alpha_p}^M = 3.1848$, $\alpha_1 = -11.3490$, $\alpha_2 = -4.3886$, $\beta_1 = -2.2936$, $\beta_2 = -5.3396$, $\gamma_1 = -0.7327$, $\gamma_2 = -0.3531$, $\gamma_\pi = -0.7993$. The *ab initio* MOs with relevance to the cluster bonding (making the target of fit in the model *Hamiltonian*) were identified selecting those with the maximal contributions to the *Mulliken* population of the cluster atoms.

With the model at hand, we can approach the estimation of the TREPE indices. For each resonance isomer r, a set of eigenvalues, e_i^r, is prepared by removing from the model *Hamiltonian* all the interatomic interactions between centers which are not connected in the corresponding graph. Then, apply Eq. (7) where e_i^d are the MO energies of the delocalized system and n_e is the number of electrons. The relatively high values (in eV, see Fig. 7d) are due to the fact that delocalization acts upon σ bonds. The narrow distribution of TREPE indices for all the isomers around the average value suggests that, in spite of topological differentiation, all the depicted structures contribute comparably to the overall resonance.

$$\mathrm{TREPE}(r) = 2\left(\sum_i^{n_e/2} e_i^d - \sum_i^{n_e/2} e_i^r\right)\Big/ n_e \tag{7}$$

The model approach illuminated the black box character of regular quantum chemical calculations and helped us touching, in the idealized model, the aromaticity keyword in the spirit of the initially mentioned idea, that the qualitative chemical meaning can be extracted from the *ab initio* schemes with help of non-standard analyses.

Acknowledgements

F. C. and *M. F.* are grateful to the Japan Society for Promotion of Science (JSPS), being also indebted to the Romanian National Council of Research (CNCSIS, grant no. 886 and 1422). "Fonds zur Förderung der Wissenschaftlichen Forschung in Österreich" (Project 15874-N03) is acknowledged, as well as JSPS for supporting the stay of *W. L.* in Japan.

References

[1] Mulliken RS (1965) J Chem Phys **S2**: 43
[2] Reed AE, Curtiss LA, Weinhold F (1988) Chem Rev **88**: 899; Glendening ED, Reed AE, Carpenter JE, Weinhold F, The NBO3.0 program
[3] Bader RFW (1990) Atoms in Molecules – A Quantum Theory. Oxford University Press, Oxford; Bader RFW (1985) Acc Chem Res **18**: 9
[4] Dapprich S, Frenking G (1995) J Phys Chem **99**: 9352
[5] Said M, Maynau D, Malrieu JP (1984) J Am Chem Soc **106**: 580; Guihery N, Benamor N, Maynau D, Malrieu JP (1996) J Chem Phys **104**: 3701
[6] Garciabach MA, Blaise P, Malrieu JP (1992) Phys Rev B-Condens Matter **46**: 15645; Capponi S, Guihery N, Malrieu JP, Miguel B, Poilblanc D (1996) Chem Phys Lett **255**: 238
[7] The calculations reported here were carried out with the GAMESS package: Schmidt MW, Baldridge KK, Boatz JA, Elbert ST, Gordon MS, Jensen JH, Koseki S, Matsunaga N, Nguyen KA, Su SJ, Windus TL, Dupuis M, Montgomery JA (1993) J Comput Chem **14**: 1347
[8] Saebo S, Pulay P (1993) Ann Rev Phys Chem **44**: 213; Schutz M, Hetzer G, Werner HJ (1999) J Chem Phys **111**: 5691
[9] Root DM, Landis CR, Cleveland T (1993) J Am Chem Soc **115**: 4201; Landis CR, Cleveland T, Firman TK (1995) J Am Chem Soc **117**: 1959
[10] Barbier C, Berthier G (2000) Adv in Quant Chem **36**: 1
[11] Nicolaides CA, Komninos Y (1998) Int J Quant Chem **67**: 321; Komninos Y, Nicolaides CA (1999) Int J Quant Chem **71**: 25

[12] Ferbinteanu M, Roesky HW, Cimpoesu F, Atanasov M, Kopke S, Herbst-Irmer R (2001) Inorg Chem **40**: 4947
[13] Wiberg KB (1986) Angew Chem Int Ed **25**: 312; Wiberg KB, Marquez M (1998) J Am Chem Soc **120**: 2932
[14] Coulson CA, Moffitt WE (1949) Philos Mag **40**: 1
[15] Reddy ND, Roesky HW, Noltemeyer M, Schmidt HG (2002) Inorg Chem **41**: 2374
[16] Reinen D, Atanasov M, Lee SL (1998) Coord Chem Rev **175**: 91; Fenton ND, Gerloch M (1990) Inorg Chem **29**: 3718; Duer MJ, Fenton ND, Gerloch M (1990) Int Rev Phys Chem **9**: 227
[17] Moesch-Zanetti NC, Hewitt M, Schneider TR, Magull J (2002) Eur J Inorg Chem 1181; Guzei IA, Winter CH (1997) Inorg Chem **36**: 4415; Guzei IA, Yap GPA, Winter CH (1997) Inorg Chem **36**: 1738
[18] King RB (2000) Coord Chem Rev **197**: 141
[19] Tanase S, Bouwman E, Reedijk J, Driessen WL, Ferbinteanu M, Mills AM, Spek AL (2004) Eur J Inorg Chem 1963
[20] Schleyer PV (2001) Chem Rev **101**: 1115
[21] Klein DJ, Trinajstić N (Ed) (1990) Valence Bond Theory and Chemical Structure. Elsevier, Amsterdam; Gerratt J, Cooper DL, Karadakov PB, Raimondi M (1997) Chem Soc Rev **26**: 87; Cooper DL, Gerratt J, Raimondi M (1991) Chem Rev **91**: 929
[22] Raimondi M, Cooper DL (1999) Top Curr Chem **203**: 105; Cooper DL, Thorsteinsson T, Gerratt J (1999) Adv Quantum Chem **32**: 51
[23] Hirao K, Nakano H, Nakayama K, Dupuis M (1996) J Chem Phys **105**: 9227; Nakano H, Sorakubo K, Nakayama K, Hirao K (2002) In: Cooper DL (ed) Valence Bond Theory. Elsevier Science, Amsterdam, p 55–77
[24] Heisenberg WZ (1928) Phys **49**: 619; van Vleck JH, Sherman A (1953) Rev Mod Phys **7**: 167; Anderson PW (1959) Phys Rev **115**: 2
[25] Cimpoesu F, Stanica N, Chihaia V, Hirao K (2003) Adv Quant Chem **44**: 273
[26] van Lenthe JH, Dijkstra F, Havenith RWA (2002) In: Cooper DL (ed) Valence Bond Theory. Elsevier Science, Amsterdam, p 79–116
[27] Mo Y, Wu W, Zhang Q (1994) J Phys Chem **98**: 10048; Janoshek R (1991) J Mol Struct (Theochem) **229**: 197; Kollmar H (1979) J Am Chem Soc **101**: 4832
[28] Glendening ED, Weinhold F (1998) J Comput Chem **19**: 593, **19**: 610; Glendening ED, Badenhoop JK, Weinhold F (1998) J Comput Chem **19**: 628; Feldgus S, Landis CR, Glendening ED, Weinhold F (2000) J Comput Chem **21**: 11
[29] Ferbinteanu M, Fukuda Y, Linert W (unpublished data)
[30] King RB (2001) Chem Rev **101**: 1119; Schleyer PV, Najafian K (1998) Inorg Chem **37**: 3454; Schleyer PV, Najafian K, Mebel AM (1998) Inorg Chem **37**: 6765
[31] Stasch A, Ferbinteanu M, Prust J, Zheng W, Cimpoesu F, Roesky HW, Magull J, Schmidt H-G, Noltemeyer M (2002) J Am Chem Soc **124**: 5441
[32] Boldyrev AI, Simons J (1998) J Am Chem Soc **120**: 7967; Li X, Zhang HF, Wang LS, Geske GD, Boldyrev AI (2000) Angew Chem Int Ed **39**: 3630
[33] Gutman I, Milun M, Trinajstić N (1977) J Am Chem Soc **99**: 1692; Graovac A, Gutman I, Randić M, Trinajstić N (1973) J Am Chem Soc **95**: 6267; Katritzky AR, Jug K, Oniciu DC (2001) Chem Rev **101**: 1421
[34] Gimarc BM, Zhao M (1996) Inorg Chem **35**: 825; Zhao M, Gimarc BM (1995) Polyhedron **14**: 1315